Progress In Electromagnetics Research C, Vol. 120, 179–193, 2022

Slotted Patch Based Multiband Antenna with Multiple DGS Effect to Suppress Cross Polarized Radiation

Rajib K. Dash*, Puspendu B. Saha, and Dibyendu Ghoshal

Abstract—A defected ground structure (DGS) loaded slotted patch antenna is proposed in this article to achieve multiband response with minimization of cross polar radiations in both the radiation planes. Besides, the antenna in this work achieves reduction in cross polar radiation at all its resonating bands with a simple inset feeding mechanism. Loading of identical U-shaped slots in the patch helps the antenna to achieve dual resonance characteristics and also leads to minimize the orthogonal E-field components. Along with the slotted patch, implementation of DGS results in multiple current paths leading to additional resonances in lower frequency range and also suppresses the strong leakage current in the ground plane. Moreover, three identical slots are loaded at the edges of the ground which balance the strong E-field components in opposite direction improving the reflection coefficient at the different resonating bands. The proposed antenna achieves multi-resonance characteristics operated in 2.44–2.56, 5.45–5.52, 6–6.13, 7.43–8.04, and 8.99–9.17 GHz. Minimization of orthogonal E-field components and suppression of leakage current are responsible for obtaining minimum cross polar radiation from the antenna as -39.08 and -41.01 dB in E- and H-planes, respectively.

1. INTRODUCTION

Radiation takes place in undesired direction from an antenna which can be considered as the cross polarization. This causes cross talk which affects the communication system seriously. Higher order orthogonal resonance which produces E-field components orthogonal to E-plane is mainly responsible for producing cross polarization. These higher order orthogonal modes are located near non-radiating edges of the patch. Different techniques have been applied in literature like shorting plates at the non-radiating edges [1], defected patch with shorting pins [2], slot made close to the shorting pin [3], and two distinct patches with array of shorting pins [4] to minimize unwanted cross polarized radiation. The introduction of defects changes the profile of the fields under the patch and disturbs the higher order resonance which reduces the orthogonal E-field components near the non-radiating edges of the patch. Along with defected patch, shorting plates and pins are employed to minimize cross polarized radiation due to orthogonal components of the dominant mode. Slot is made close to the shorting pin to reduce cross polarization level by diverting current along the width.

Apart from shorting plates and pins, different additional mechanisms such as anisotropic substrate to introduce additional cross polarized fields of opposite phase in order to cancel the cross polarized field produced in patch [5], spiral ring resonators loaded 2×2 antenna array consisting of E-shaped patch [6], slotted cavity enclosed balun fed printed dipole antenna [7], and coupled fed antenna with vias, stubs, and metallic shield [8] have been implemented to reduce cross polarized radiation. An antenna array consisting of E-shaped patch produced a single band response within a band range of 5.175–5.580 GHz.

Received 17 March 2022, Accepted 17 May 2022, Scheduled 3 June 2022
* Corresponding author: Author Name (rkdashece@gmail.com).
The authors are with the Department of Electronics and Communication Engineering, National Institute of Technology, Agartala 799046, India.

Implementation of vias, stubs, and metallic shield produced radiation nulls to reduce cross polarized radiation.

Different defected ground structure (DGS) techniques like elliptical DGS in a simple patch antenna producing a single band response with the reduction of cross polarization level by 16–18 dB [9], etching a notch at the edge of the ground plane, loading of an array of slots at left ground plane, implementation of inverted U-shaped strips at the top of the substrate for minimization of unbalanced horizontal currents reducing cross polarization up to 19 dB [10], Z-shaped slot in the ground plane of a rectangular patch antenna producing less cross polarization in H-plane around 22 dB within the operating band range 2.38–2.58 GHz [11], two slots etched in the ground plane in order to couple the weak fields resulting in less leakage current in the ground to achieve reduction in cross polarized radiation around 10–20 dB [12], loading of L-shaped DGS in a circular polarized microstrip patch reducing cross polarization up to −27.49 dB due to minimization of higher order orthogonal modes [13], etc. have been reported in literature.

Alongside reduction in cross polarization level, efforts have also been given to designing antenna with multiband behavior implementing different mechanisms like incorporation of slots with different shapes at different position in the patch [14–16], implementation of three identical slots in ground plane to produce resonance in lower frequency range [17], an inset fed patch antenna embedded with two slotted parasitic elements to achieve additional bands and additional square shapes to suppress back lobe radiation [18], and loading of different shaped slots in the ground plane of a slotted patch [19] from a simple microstrip patch.

An inset fed U-shaped slotted patch and multiple DGSs in ground is designed and presented in this article to realize a multiband antenna with reduced cross polarized radiation at each of its resonating bands. During the entire design process, simulation of each design stage is done using HFSS, and finally a multiband response is obtained with the reduction in cross polarized radiation. Apart from this, the proposed antenna in the final stage achieves improved gain, better reflection coefficient, and desired radiation patterns. Different design parameters of the proposed antenna are optimized properly to get improvement in antenna performance using parametric analysis, and the validation of simulated outcomes of the proposed design is done by comparing with the measurement results of the fabricated prototype. The proposed antenna in its final form is depicted in Figure 1.

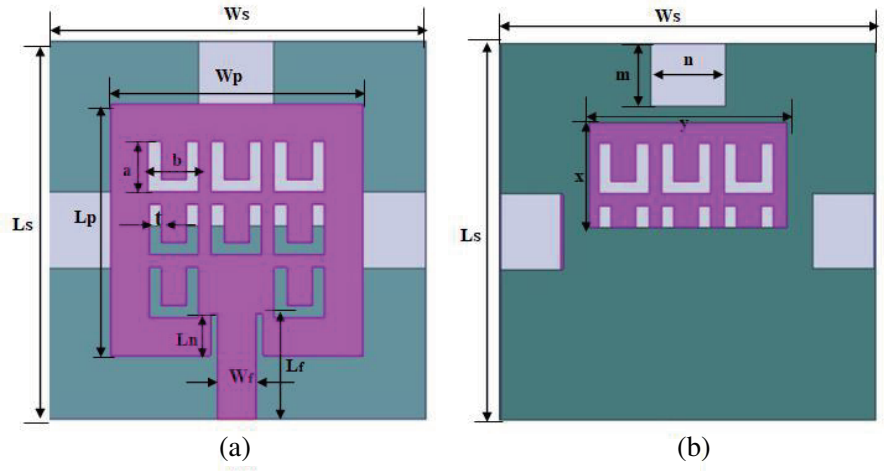

Figure 1. Proposed antenna. (a) Front view. (b) Bottom view.

In this article, various techniques are implemented to improve the performance of a conventional microstrip patch antenna such as implementation of slots and DGS in its patch and ground plane respectively to achieve multi-resonance behavior with the minimization of cross polarization at all its bands of resonance. The proposed antenna in this design is very simple and compact avoiding complex feeding mechanism and difficult fabrication process without offering back radiation. It produces less cross polarized radiation at all its resonating bands whereas most of the designs in literature are limited to the reduction of cross polar radiation at single resonating band only.

2. DESIGN PRINCIPLE

Antenna structure involves a square patch with U-shaped slots and ground plane consisting of multiple defects as shown in Figure 1. The U-slots loaded patch with design specifications $\mathbf{W_p}$ and $\mathbf{L_p}$ is mounted on an FR4 epoxy substrate of dimensional parameters $\mathbf{W_s}$ and $\mathbf{L_s}$ as given in Figure 1. Dielectric constant and the loss tangent of the substrate are 4.4 and 0.02, respectively. The feedline with proper specifications $\mathbf{W_f}$ and $\mathbf{L_f}$ is connected through the feeding slot of length $\mathbf{L_n}$ to achieve 50 Ohm impedance matching. The length and width of each U-shaped slot are **a** and **b** respectively with thickness **t** as shown in Figure 1(a). Ground plane consists of a rectangular slot of length **x** and width **y** at bottom of the substrate to achieve desired resonances in lower range. Three identical additional slots of length **m** and width **n** are loaded at the edges of the ground plane as shown in Figure 1(b) to improve the resonance characteristics of the proposed antenna. Detailed dimensional specifications with values of the proposed antenna are shown in Table 1.

Table 1. Design specification of the proposed antenna.

Parameters	Values (mm)	Parameters	Values (mm)	Parameters	Values (mm)
$\mathbf{W_s}$	30	$\mathbf{W_f}$	3	**x**	10
$\mathbf{L_s}$	30	$\mathbf{L_f}$	7.6	**y**	16
$\mathbf{W_p}$	20	**a**	4	**m**	5
$\mathbf{L_p}$	20	**b**	4	**n**	6
$\mathbf{L_n}$	2.6	**t**	1	**-**	-

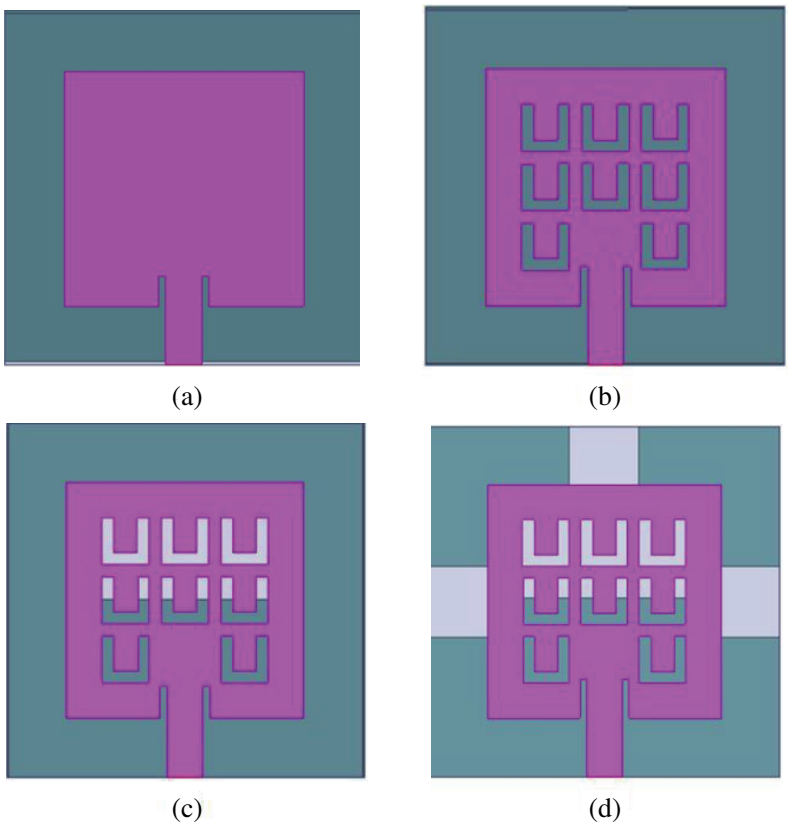

Figure 2. Design stages. (a) Stage-1. (b) Stage-2. (c) Stage-3. (d) Stage-4.

Initially, an inset fed square-shaped patch is taken into consideration to establish proper impedance matching. For this, a small slot has been made at the lower edge of the patch known as the feeding slot. Then the feedline with proper specification is connected to the patch through the feeding slot as shown in Figure 2(a). In inset feeding mechanism, it is very important to determine the location of the exact feeding point. Parametric analysis is carried out to determine the exact location of feeding by setting slot length (Ln) as a variable. Since the conventional patch antenna is meant for single band resonance, U-shaped slots are loaded on the patch as shown in Figure 2(b) to obtain additional frequency bands. U-shaped slots of equal size and shapes loaded patch causes significant disturbances in E-field distribution below the patch which increases current along the edge and decreases through the surface. This leads to obtaining more frequency bands with additional gain of the designed antenna. U-shaped slotted patch produces one additional resonance in higher frequency range.

In order to achieve more frequency bands within desired lower frequency range, ground plane is loaded with a slot at bottom of the substrate as shown in Figure 2(c). The implementation of DGS causes significant disturbances in E-field around the ground plane and results in the increase in E-field distribution at the edges of the slots and upper edge of the ground plane as shown in Figure 4(d). At the same time, there is a decrease in electric field at the lower portion of the ground plane. Thus, DGS generates multiple current paths leading to multiband resonance. The slotted patch with single DGS produces multiband response; however, it has been observed that most of the bands suffer with higher reflection coefficient. In order to improve the reflection coefficient, three additional DGSs have been implemented at each side of the ground plane except the lower edge as shown in Figure 2(d). It neutralizes the strong electric field components in reverse direction which causes improvement in reflection coefficient. The size of the slots in ground plane is optimized using parametric analysis.

3. PARAMETRIC ANALYSIS

3.1. Variation in Ln

Inset feeding mechanism has been implemented in order to get proper impedance matching. To achieve this, the patch is loaded with a feeding slot. In order to create 50 Ohm impedance matching width of the feedline is kept fixed, whereas the feedline length is decided from the proper feeding location. Length of the feeding slot (Ln) is treated as a variable to perform parametric analysis within the range 2.2–3 mm in a gap of 0.2 mm. It has been observed that reflection coefficient decreases with the increase in Ln, being minimum at Ln = 2.6 mm and again increases beyond Ln = 2.6 mm as shown in Figure 3(a).

3.2. Variation in x

Ground is loaded with a rectangular slot of length x to ensure multiband response. To determine the suitable value of x, a parametric variation is done by considering x as a variable while y is kept constant. Variation is performed within 6–14 mm with a step size of 2 mm. It has been noticed that antenna generated triple resonance behavior at $x = 6$ and 8 mm, whereas most of the bands occurred in higher range of frequency. As x increases beyond 8 mm, additional bands have been achieved, ensuring improvement in multi-resonance characteristics of the antenna at $x = 10$ and 12 mm. It has been noted that at $x = 10$ mm, multiband response is obtained with minimum reflection coefficient in comparison to $x = 12$ mm as shown in Figure 3(b). It has been observed that beyond $x = 12$ mm, there is a decrease in multiband behavior of the antenna.

3.3. Variation in y

Parametric variation of y is performed between 12 and 20 mm with the step size of 2 mm as shown in Figure 3(c). At the same time, x is kept fixed. Y is the width of the rectangular slot which is loaded in the ground to achieve multiband response. It has been shown that dual-band response is obtained from the antenna at $y = 12$ and 14 mm. As y increases beyond 14 mm, more resonating bands are generated in the desired range of frequencies ensuring the multiband response of the antenna at $y = 16$ mm with considerable reflection coefficient. Afterward, there is a degradation in the multiband performance of the antenna.

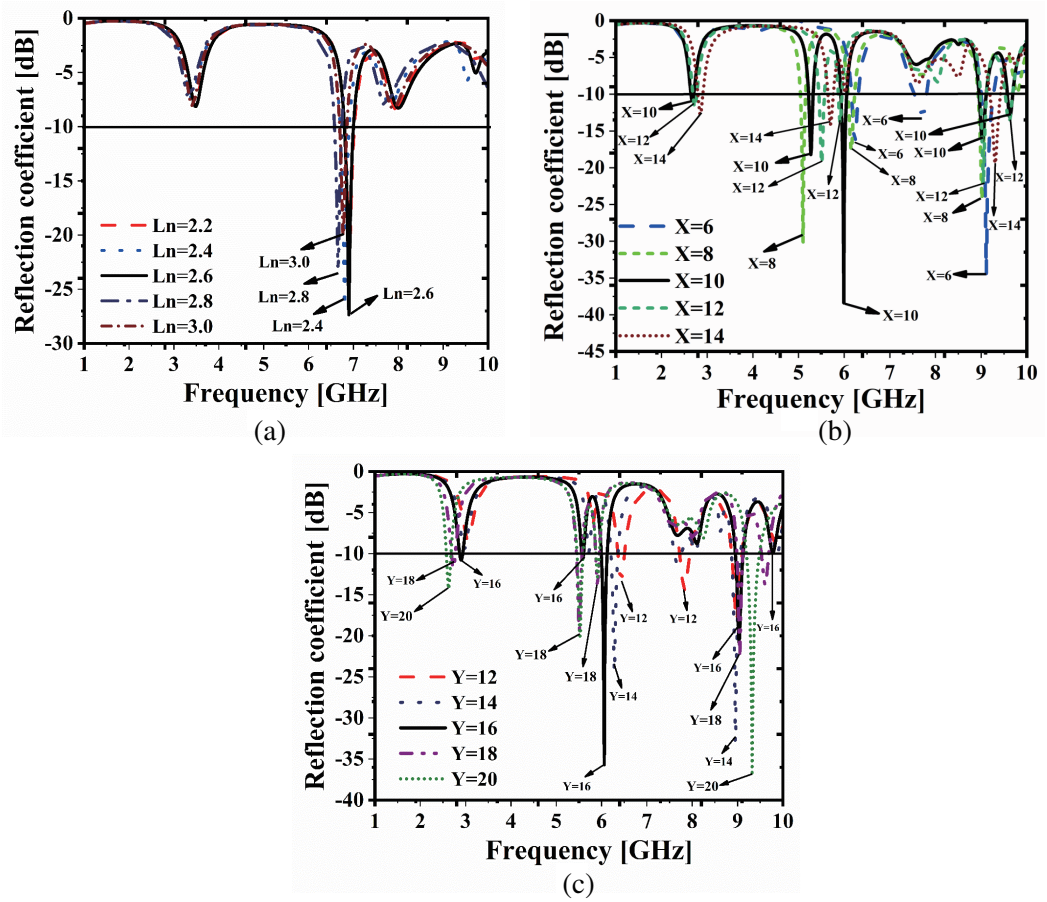

Figure 3. Parametric analysis. (a) Variation in Ln. (b) Variation in X. (c) Variation in Y.

4. REDUCTION IN CROSS POLARIZED RADIATION

Orthogonal E-field components corresponding to higher order resonant modes are the primary source of cross polarized radiations usually located near the non-radiating edges of the patch [20]. Figure 4(a) describes E-field distributions in the patch without slots. The presence of orthogonal modes can be observed near the non-radiating edges of the patch. E-field distribution of the ground plane without DGS is shown in Figure 4(b). It can be observed that most of the E-field components concentrate at the lower portion of the ground which produce more leakage current with more cross polarized radiations. In this work, the effect of defected ground structure and slotted patch implemented in the design are utilized to suppress the cross polarization in both E- and H-planes. Significant disturbances in fields occur below the patch due to the presence of slots changing the radiation behavior of the designed antenna. It leads to the minimization of orthogonal E-field components near the non-radiating edge by cancelling the higher order modes as shown in Figure 4(c). At the same time, E-field components at the radiating edge which are responsible for co-polarization are not affected. The implementation of a rectangular slot at the surface and three identical rectangular slots at the edges of the ground plane reduces cross-polarized radiation. DGS effect in the edge along with surface of the ground plane significantly disturbs the field which in turn leads to minimizing the field components at lower part and suppresses the strong leakage current. Thus, it results in the decrease in cross-polarized radiation. At the same time, the slot in the surface is used to neutralize part of the field components outflowing from the patch which lead to the decrease in cross-polarized radiation. Figure 4(d) shows the E-field distributions along the ground plane with DGS effect.

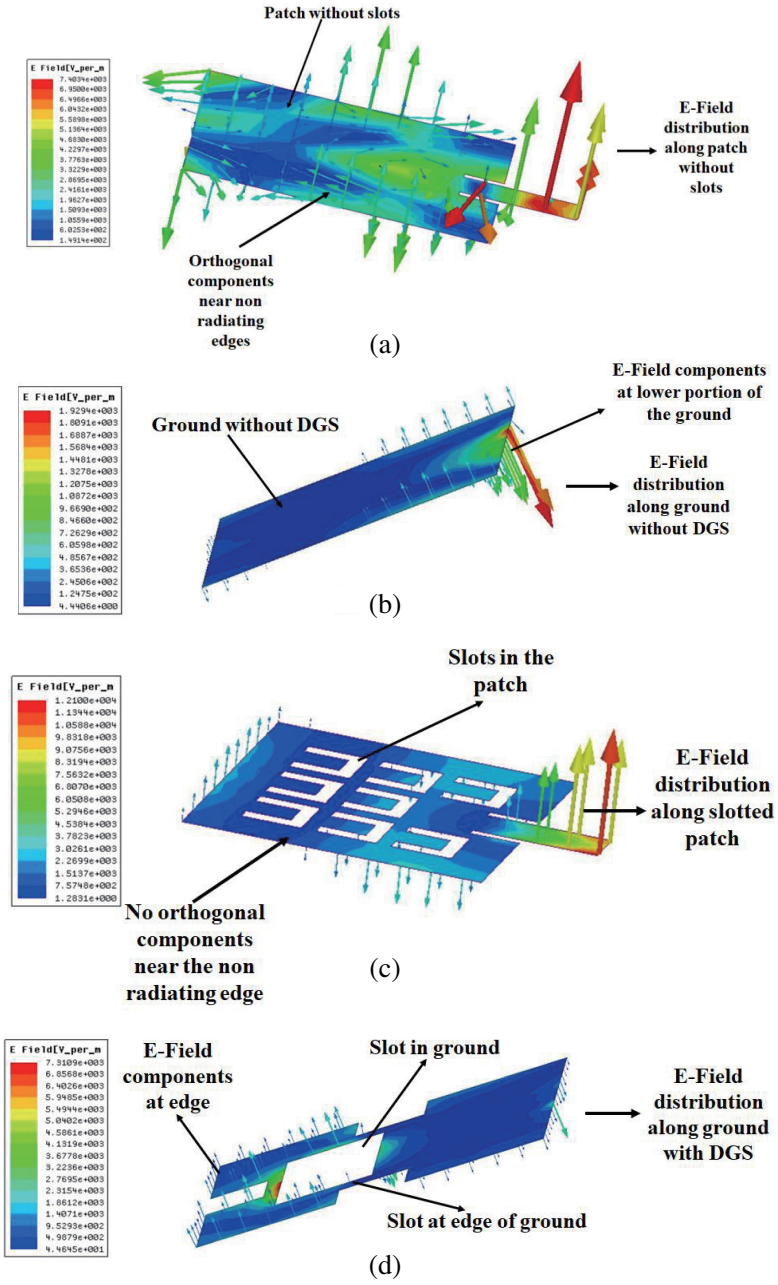

Figure 4. *E*-field distribution. (a) Patch without slots. (b) Ground without DGS. (c) Slotted patch. (d) Ground with DGS.

5. RESULTS AND DISCUSSION

5.1. Reflection Coefficient and Bandwidth

This context describes the results of reflection coefficients and bandwidth of the designed antenna. The antenna is fabricated and then tested through Rhode and Schwarz ZNB 20 vector network analyzer (VNA) whose operating frequency lies between 100 KHz and 20 GHz. A simple square-shaped patch fed through inset feeding mechanism produces a reflection coefficient of −32.77 dB, operating within 6.78–6.96 GHz at a resonance of 6.87 GHz. A U-shaped slotted patch resonates at 6.29 and 9.02 GHz with reflection coefficients −17.51 and −24.89 dB, respectively. In this stage, the antenna produces

bandwidths of 120 MHz (6.23–6.35 GHz) and 190 MHz (8.93–9.12 GHz). The DGS implemented U-shaped slotted patch has generated multiband response with reflection coefficients −13.93, −23.70, −15.04, −13.53, and −12.06 dB corresponding to resonances 2.75, 5.47, 5.9, 9.05, and 9.6 GHz, respectively. The bandwidths produced in this stage are 110 MHz (2.69–2.80 GHz), 120 MHz (5.41–5.53 GHz), 80 MHz (5.86–5.94 GHz), 120 MHz (8.99–9.11 GHz), and 120 MHz (9.54–9.66 GHz).

Finally, the antenna design is implemented with a U-shaped slotted patch with multiple DGSs in ground and produces simulated reflection coefficients of the proposed antenna −16.59, −15.40, −35.54, −18.30, and −25.99 dB with resonant frequencies 2.5, 5.49, 6.06, 7.71, and 9.08 GHz, respectively. The bandwidths produced in this range are 120 MHz (2.44–2.56 GHz), 70 MHz (5.45–5.52 GHz), 130 MHz (6.0–6.13 GHz), 610 MHz (7.43–8.04 GHz), and 180 MHz (8.99–9.17 GHz). Reflection coefficients variations in different stages are shown in Figure 5(a). The comparison of measured and simulated reflection coefficients of the proposed antenna is shown in Figure 5(b). Measured reflection coefficients are found to be −13.66, −16.43, −31.66, −13.39, and −23.92 dB at frequencies 2.55, 5.46, 6, 7.62, and 9.02 GHz produced by this antenna. The antenna operates within the range (2.49–2.62), (5.41–5.50), (5.95–6.07), (7.46–7.94), and (8.95–9.09) GHz corresponding to each resonance. A slight difference is between simulated and measured outcomes because of the tolerance in fabrication. Table 2 shows all the resonances along with their operating bands and reflection coefficients of the different design stages.

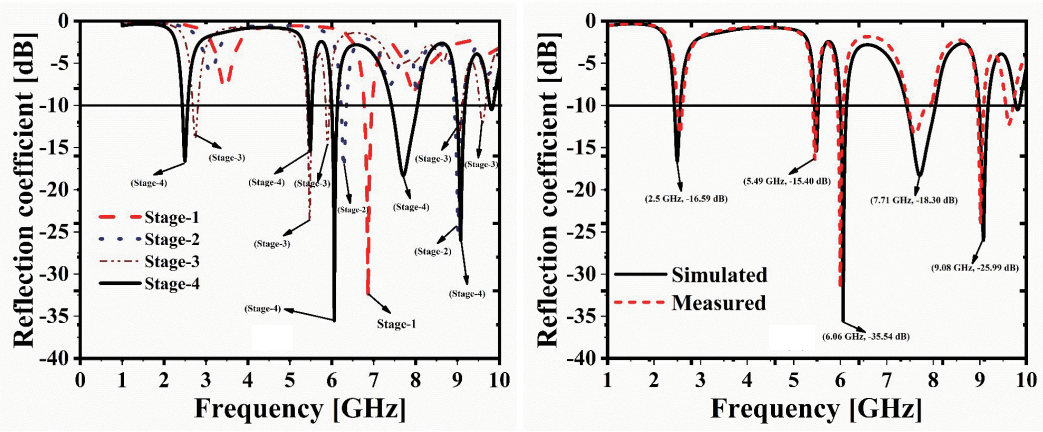

Figure 5. Reflection coefficient variation in (a) all stages (b) simulated and measured values of the antenna.

Table 2. Resonance characteristics of all design stages of the proposed antenna.

Stages	Resonant frequency (GHz)	Reflection coefficients (dB)	Bandwidth (MHz)
Stage-1	6.87	−32.77	180
Stage-2	6.29, 9.02	−17.51, −24.89	120, 190
Stage-3	2.75, 5.47, 5.9, 9.05, 9.6	−13.93, −23.70, −15.04, −13.53, −12.06	110, 120, 80, 120, 120
Proposed antenna (Simulated)	2.5, 5.49, 6.06, 7.71, 9.08	−16.59, −15.40, −35.54, −18.30, −25.99	120, 70, 130, 610, 180
Proposed antenna (Measured)	2.55, 5.46, 6, 7.62, 9.02	−13.36, −16.43, −31.66, −13.39, −23.92	130, 90, 120, 480, 140

5.2. Radiation Pattern and Polarization

Radiation pattern of the antenna describes the mechanism of dissipating energy in space. Dissipation of energy is usually expressed as a function of direction. Radiation patterns of the proposed antenna from simulation and measurement at different resonances are exhibited in Figure 6. It shows that the antenna produces almost omnidirectional radiation at 2.5 GHz and nearly omnidirectional at 5.49 GHz in H-plane as shown in Figures 6(a) and 6(b). At the same time, nearly bidirectional H-plane pattern is obtained at all other resonant frequencies of the proposed antenna as shown in Figures 6(c–e). It has been observed that radiation pattern is nearly bidirectional in E-plane at frequencies 2.5 and 7.71 GHz resulting from the proposed antenna as shown in Figures 6(a) and 6(d). Radiation patterns in E-plane

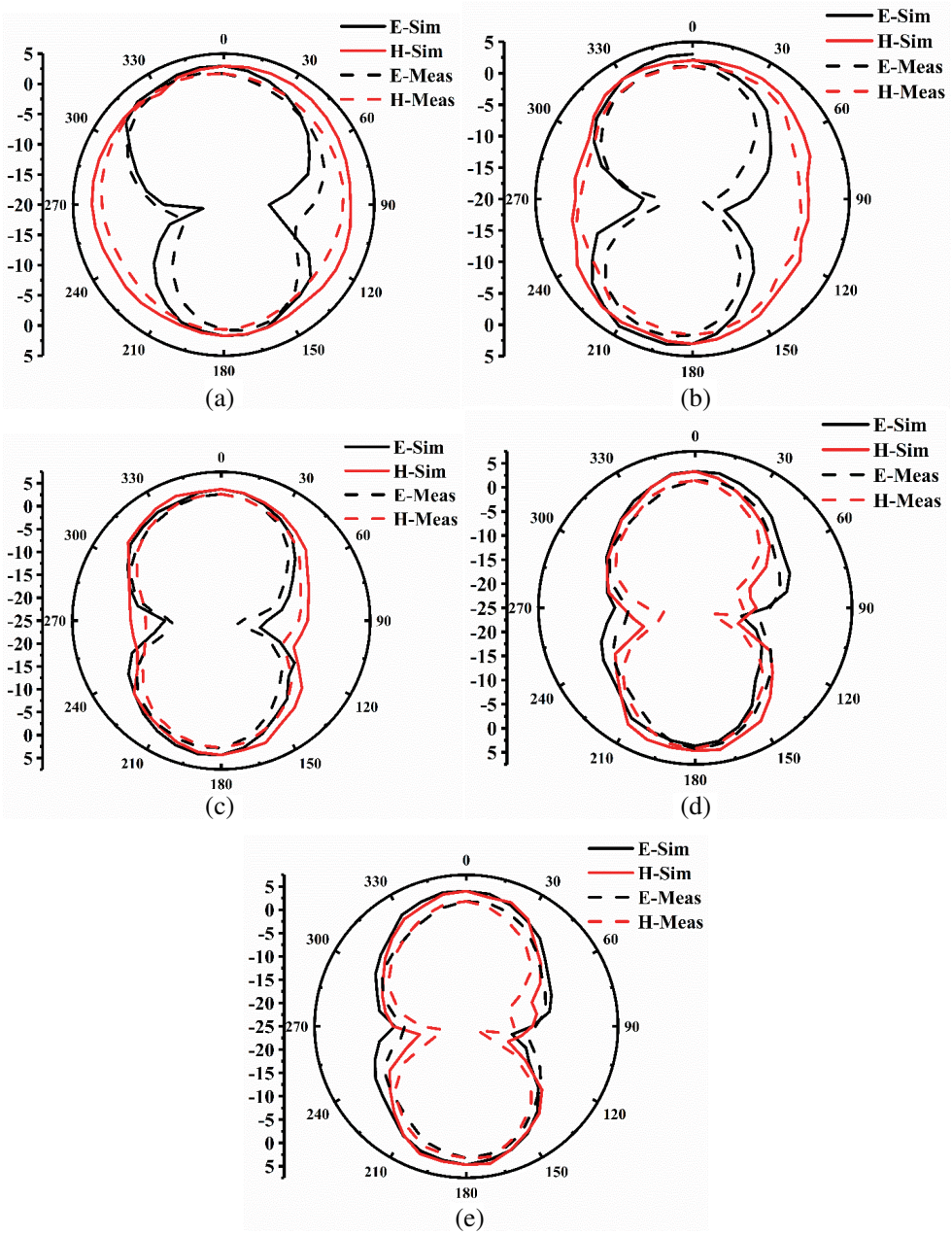

Figure 6. Simulated and measured radiation patterns at (a) 2.5 GHz (b) 5.49 GHz (c) 6.06 GHz (d) 7.71 GHz (e) 9.08 GHz.

for all other resonances of the given antenna are almost bidirectional in nature as shown in Figures 6(b), 6(c), and 6(e).

Cross polarization describes the radiations from the antenna in undesired direction. Reduction in cross polarized radiations ensures improvement in radiation performance of the antenna. Simulated and measured co- and cross-polarizations in E-plane for all resonant frequencies are shown in Figure 7. It has been observed that co-polarized gains obtained from the antenna are 1.80, 3.04, 4.43, 2.44, and 2.60 dB corresponding to each resonance, whereas cross-polarized gains produced from the antenna are −19.75, −33.23, −39.08, −29.34, and −38.83 dB corresponding to all the resonating bands. Table 3 describes the E-plane co- and cross-polarizations of the proposed antenna at principal radiating direction. It has been noted that co-polar radiation is more than the cross-polar radiation through the entire angular range for all resonating bands. Cross-polarized radiations in E-plane are kept below the co-polarization by −21.55 dB, −36.27 dB, −43.51 dB, −31.78 dB, and −41.43 dB respectively at principal radiating

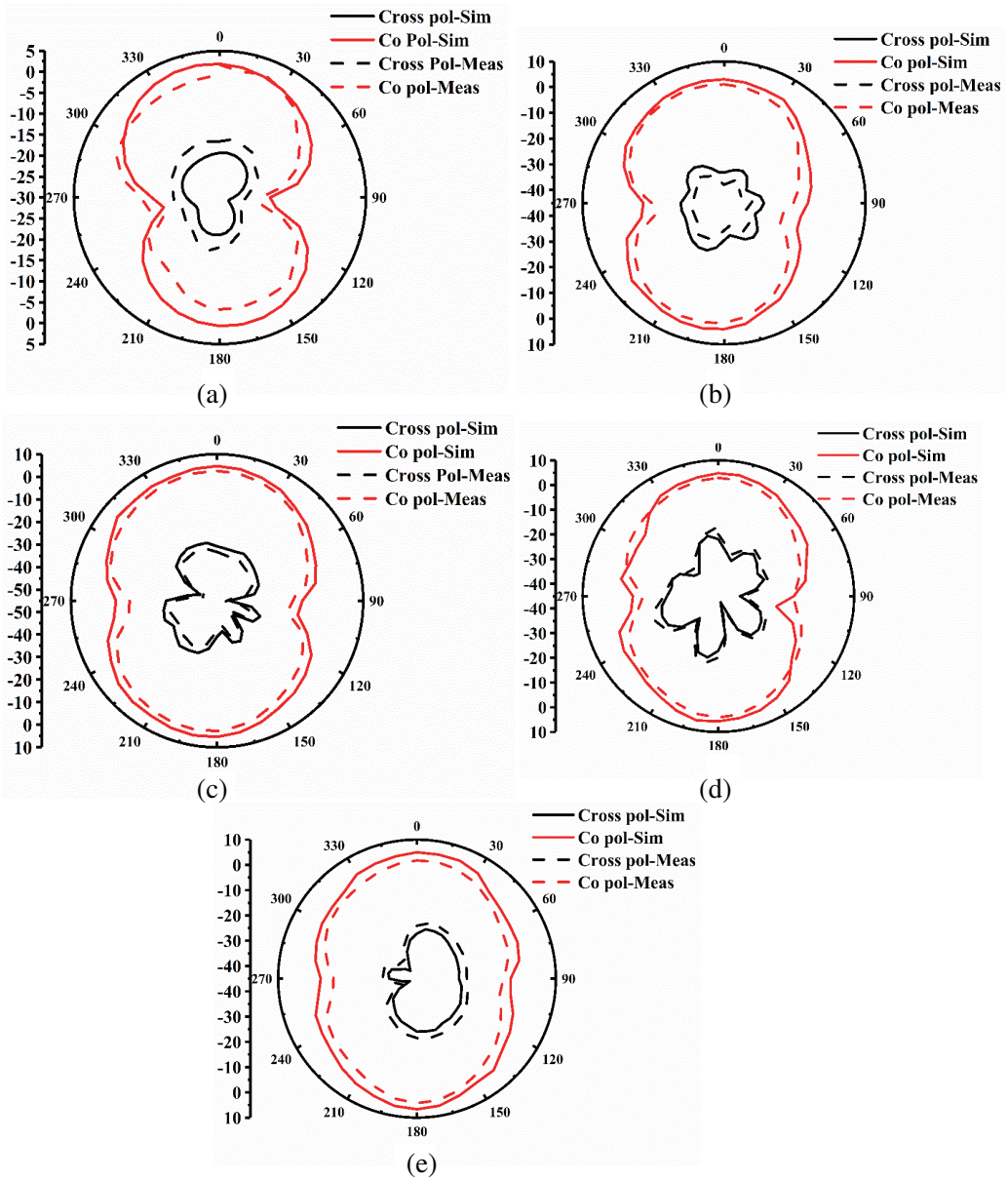

Figure 7. Simulated and measured co and cross polarization in E-plane at (a) 2.5 GHz (b) 5.49 GHz (c) 6.06 GHz (d) 7.71 GHz (e) 9.08 GHz.

direction for different resonating bands.

H-plane co- and cross-polarizations from simulation and measurement for all the resonances are depicted in Figure 8. It has been observed that co-polarized gains obtained from the antenna are 3.12, 2.93, 2.93, 3.34, and 4.28 dB corresponding to each resonance, whereas cross-polarized gains produced from the antenna are −39.33, −38.74, −41.01, −38.83, and −37.01 dB corresponding to all the resonating bands. Table 4 describes the H-plane co- and cross-polarizations of the proposed antenna at principal radiating direction. It has also been noticed that co-polar radiation is above the cross-polar radiation through the entire angular range for all resonating bands. It is kept below the co-polarization by −42.45, −41.67, −43.94, −42.17, and −41.29 dB respectively at principal radiating direction for all resonating bands. It is observed that outcomes from both simulation and measurement are very much similar to each other.

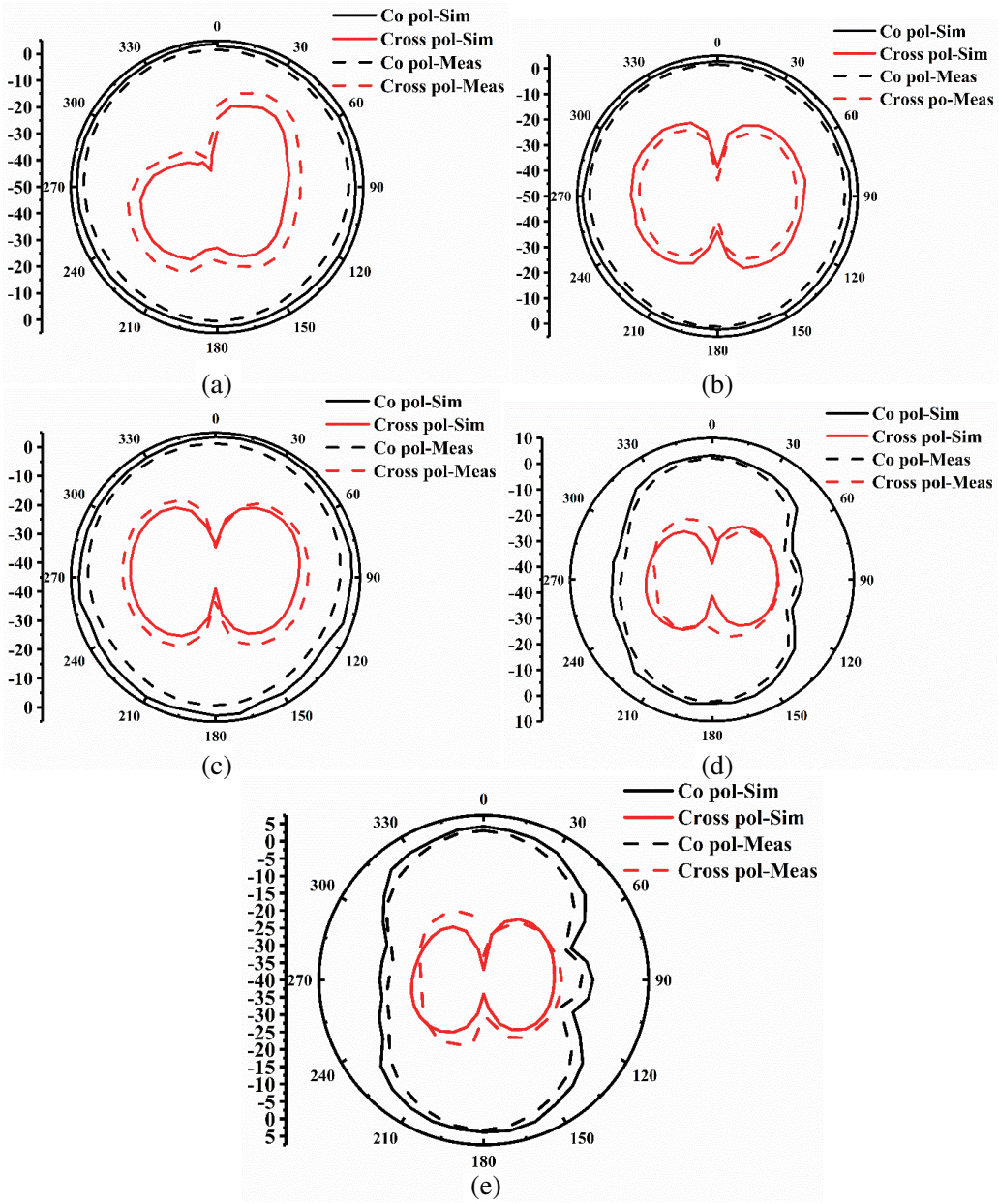

Figure 8. Simulated and measured co and cross polarization in H-plane at (a) 2.5 GHz (b) 5.49 GHz (c) 6.06 GHz (d) 7.71 GHz (e) 9.08 GHz.

Table 3. *E*-plane co- and cross-polarizations of the proposed antenna at principal radiating direction.

Resonant frequency (GHz)	Simulated Co pol gain (dB)	Measured Co pol gain (dB)	Simulated Cross pol gain (dB)	Measured cross pol gain (dB)
2.5	1.80	1.52	−19.75	−16.62
5.49	3.04	2.15	−33.23	−37.93
6.06	4.43	2.78	−39.08	−42.77
7.71	2.44	1.37	−29.34	−27.71
9.08	2.60	1.58	−38.83	−35.20

Table 4. *H*-plane co- and cross-polarizations of the proposed antenna at principal radiating direction.

Resonant frequency (GHz)	Simulated Co pol gain (dB)	Measured Co pol gain (dB)	Simulated Cross pol gain (dB)	Measured cross pol gain (dB)
2.5	3.12	1.54	−39.33	−34.96
5.49	2.93	1.66	−38.74	−43.70
6.06	2.93	1.57	−41.01	−37.18
7.71	3.34	2.22	−38.83	−25.65
9.08	4.28	3.05	−37.01	−33.05

5.3. Gain and Radiation Efficiency

Variation of the simulated gain and efficiency with their measured equivalent outcomes resulting from the proposed antenna over the entire frequency range is performed towards realization of both gain and radiation efficiency in the operation band as shown in Figure 9. It has been shown that variations of both the parameters obtained from simulation and measurement are very much relatable with each other. Peak gains obtained from the antenna are 3.07, 3.04, 4.57, 4.88, and 4.90 dB corresponding to different resonances as shown in Figure 9(a), whereas the corresponding radiation efficiencies are 67.67%, 65.26%, 75.49%, 98.43%, and 86.67% at the different frequencies of resonance as shown in Figure 9(b). Table 5 describes the values of gain and radiation efficiencies obtained from both simulation and measurement of the proposed antenna at different resonant frequencies.

The proposed antenna in this design uses an FR4 substrate due to some significant properties like ease of availability, inexpensive towards cost effectiveness, robust in different environmental conditions

Table 5. Gain and radiation efficiency of the proposed antenna.

Resonant frequency (GHz)	Simulated gain (dB)	Measured gain (dB)	Simulated efficiency (%)	Measured efficiency (%)
2.5	3.07	1.89	67.67	69.57
5.49	3.04	1.76	65.26	59.87
6.06	4.57	2.65	75.49	69.6
7.71	4.88	3.79	98.43	82.45
9.08	4.90	3.55	86.67	86.63

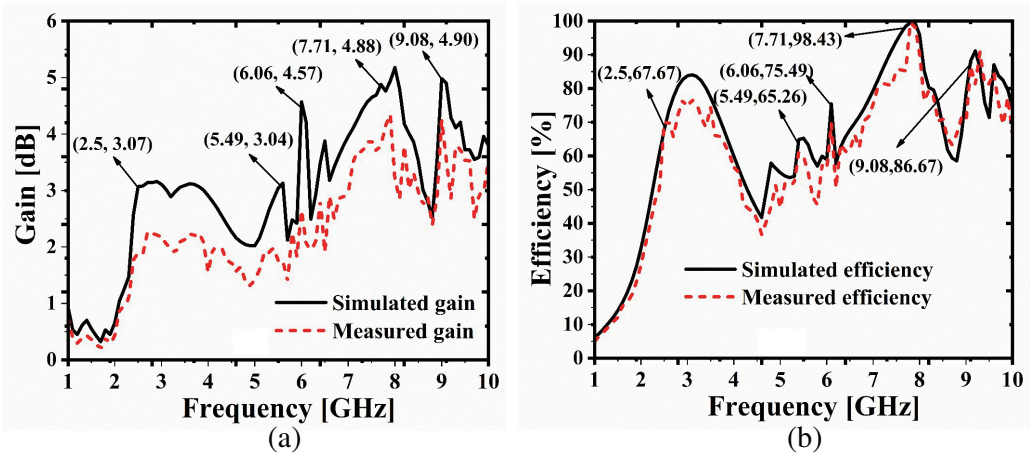

Figure 9. Comparison of simulated and measured. (a) Gain vs Freq. (b) Efficiency vs Freq of the proposed antenna.

because of its ability in resistance against different temperatures and high degree of electrical and mechanical stability. Apart from these advantages, it mostly affects the gain of the antenna in higher range of frequencies due to its lossy nature which is the major limitation of FR4 substrate. In this work, the performance of the proposed antenna such as gain and radiation efficiencies is compared with two different substrate materials as FR4 and a low loss RT duroid material. The variation of the gain and radiation efficiency of the proposed antenna with two different substrates have been performed in simulation, and their comparison is shown in Figure 10. It has been observed that antenna with an RT duroid substrate results in more gain and radiation efficiencies than FR4 substrate; however, the amount of gain and radiation efficiencies obtained from antenna with FR4 material can be still considered in various wireless applications. It can also be noted that in higher frequency range, the variations of both gain and radiation efficiency of the antenna are very much comparable for both kinds of substrate materials. It is possible because of the minimization of back lobe radiations from the antenna of FR4 material with the introduction of slots at the edges of the ground plane.

Fabricated prototype of the proposed antenna is shown in Figure 11. Comparison of the designed antenna with different existing works is shown in Table 6. It has been shown that the isolation between co- and cross-polarizations is around 22–44 dB in E-plane and 18–43 dB in H-plane produced by the antenna through the entire angular span.

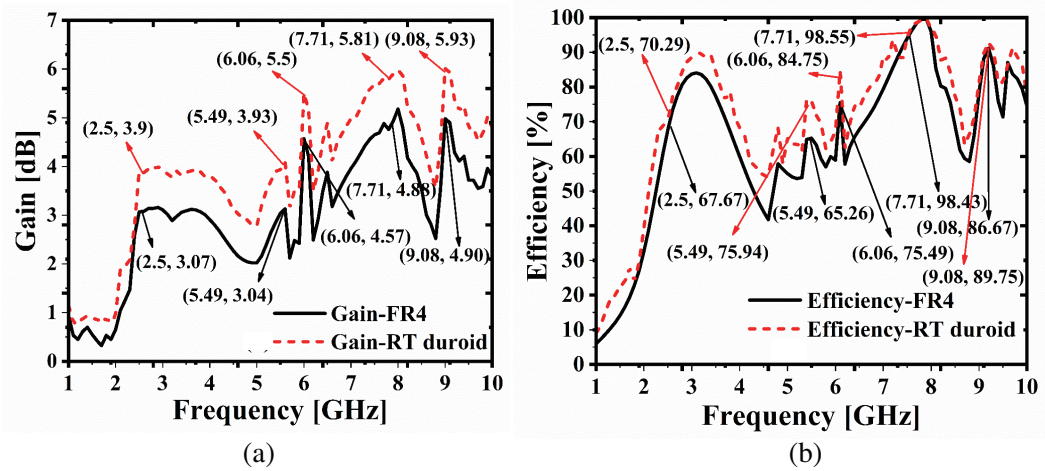

Figure 10. Comparison of effects of FR4 and RT duroid substrate on (a) Gain (b) Radiation efficiency in the proposed antenna.

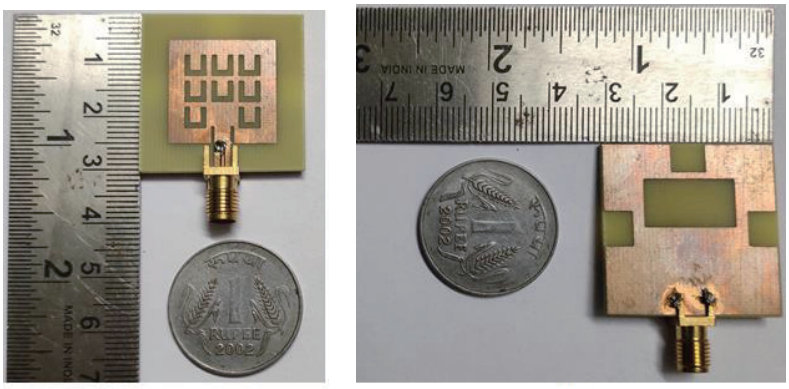

(a) (b)

Figure 11. Fabricated prototype. (a) Front view. (b) Bottom View.

Table 6. Comparison of the designed antenna with different existing works.

References	Antenna size (mm^2)	Nature	Cross-pol reduction technique	Cross-pol reduction level (dB)
[3]	53.47×44.05	Single band	DPS with shorting pin	−30
[4]	125×200	Dual band	Array of shorting pins	−23.5
[5]	70×70	Single band	Anisotropic substrate	−28
[6]	80×74.2	Single band	Spiral SRR	−12
[8]	31×31	Dual band	Vias, stubs, metallic shield	−25
[10]	50×60	Single band	Array of slots	−19.08
[11]	38×47	Single band	Z-shaped DGS	−22
[12]	68×68	Single band	Slots in ground	10–20
[13]	59.5×64.5	Single band	L-shaped DGS	−27.49
Proposed design	**30×30**	**Penta band**	**Defected patch with multiple DGS**	−43.94

6. CONCLUSION

A U-shaped slots loaded patch antenna integrated with multiple DGS effect is designed and realized to achieve reduction in cross polarization at all its resonating bands in E- and H-planes. The proposed antenna generates narrow bandwidths at all resonating bands which eliminate the need of frequency selective circuits and filters at the receiving side. Lowering of cross-polar radiations and multiband response is obtained with less cross-polarized radiation due to the implementation of U-shaped slots in patch and multiple DGS in ground. Fabricated prototype of the antenna is tested, and it has been compared with several existing works. Results from simulation and measurement have been compared, and they are very much identical to each other. Outcomes from the antenna are very much suitable for different applications including fixed point to point useing broadband service by legacy educational licenses (2.5 GHz), WiMAX (5.5 GHz), IEEE802.11ax for Wi-Fi (6.06 GHz) and X-band satellite applications.

REFERENCES

1. Poddar, R., S. Chakraborty, and S. Chattopadhyay, "Improved cross polarization and broad impedance bandwidth from simple single element shorted rectangular microstrip patch: theory and experiment," *Frequenz*, Vol. 70, No. 1–2, 1–9, DOI 10.1515/freq-2015-0105, 2016.
2. Ghosh, A., S. Chattopadhyay, L. L. K. Singh, et al., "Wide bandwidth microstrip antenna with defected patch surface for low cross polarization applications," *Int J RF Microw Comput Aided Eng.*, e21127, https://doi.org/10.1002/mmce.21127, 2017.
3. Singh, A., S. Vijay, and R. N. Baral, "Low cross-polarization improved-gain rectangular patch antenna," *Electronics*, Vol. 8, 1189, doi:10.3390/electronics8101189, www.mdpi.com/journal/electronics, 2019.
4. Liu, N., S. Gao, L. Zhu, et al., "Low-profile microstrip patch antenna with simultaneous enhanced bandwidth, beamwidth, and cross-polarization under dual resonance," *IET Microw. Antennas Propag.*, Vol. 14, No. 5, 360–365, The Institution of Engineering and Technology, 2020.
5. Shi, H., S. Zhu, J. Li, et al., "Cross-polarization suppression in C-shaped microstrip patch antenna employing anisotropic dielectrics," *Journal Of Advanced Dielectrics*, Vol. 7(4), 1750026 (5 pages), DOI: 10.1142/S2010135X17500266, 2017.
6. Ghosh, C. K., B. Rana, and S. K. Parui, "Reduction of cross polarization of slotted microstrip antenna array using spiral-ring resonator," *Microwave and Optical Technology Letters*, Vol. 55, No. 9, DOI 10.1002/mop, 2013.
7. Huang, H., X. Zhang, S. Xie, W. Wu, and N. Yuan, "Suppression of cross-polarization of the microstrip integrated balun-fed printed dipole antenna," *Hindawi Publishing Corporation International Journal of Antennas and Propagation*, Vol. 2014, 8 pages, Article ID 765891, http://dx.doi.org/10.1155/2014/765891, 2014.
8. Meng, C., J. Shi, and J. Chen, "Flat-gain dual-patch antenna with multi-radiation nulls and low cross-polarization," *Electronics Letters*, Vol. 54, No. 3, 114–116, 2018.
9. Heydari, R. D. and N. Moghadasi, "Introduction of a novel technique for the reduction of cross polarization of rectangular microstrip patch antenna with elliptical DGS," *Journal of Electromagnetic Waves and Applications*, Vol. 22, No. 8–9, 1214–1222, DOI: 10.1163/156939308784158788, 2008.
10. Wang, C. J., "Methods of suppression of cross-polarized power for the CPW-fed monopole antenna," *Microw Opt Technol. Lett.*, Vol. 59, 1968–1975, https://doi.org/10.1002/mop.30657, 2017.
11. Acharjee, J., A. K. Singh, K. Mandal, et al., 2019, "Defected ground structure toward cross polarization reduction of microstrip patch antenna with improved impedance matching," *Radio Engineering*, Vol. 28, No. 1, DOI: 10.13164/re.2019.0033, April 2019.
12. Khouser, H. and Y. K. Choukiker, "Cross polarization reduction using DGS in microstrip patch antenna," *International conference on Microelectronic Devices, Circuits and Systems (ICMDCS)*, 10–12, August 2017, Vellore, India, DOI: 10.1109/ICMDCS.2017.8211577, 2017.
13. Anita, R. and M. V. Kumar, "Cross polarization reduction of a circular polarized microstrip antenna with two L slot DGS for wireless applications," *International Journal of Pure and Applied Mathematics*, Vol. 120, No. 6, 1173–1188, 2018.
14. Dash, R. K., P. B. Saha, and D. Ghoshal, "Design of a equally spaced u shaped slotted patch antenna with defected ground structure for multiband applications," *7th International Conference on Signal Processing and Integrated Networks (SPIN)*, Noida, India, DOI: 10.1109/SPIN48934.2020.9071199, February 27–28, 2020.
15. Badr, S. and K. I. Ehab, "Design of multiband microstrip patch antenna for WiMax, C-band and X-band applications," *Aswan Engineering Journal (AswEJ)*, https://www.researchgate.net/publication/324597715, 2018.
16. Kaushal, D. and T. Shanmuganantham, "A Vinayak slotted rectangular microstrip patch antenna design for C-band applications," *Microw. Opt. Technol. Lett.*, Vol. 59, 1833–1837, https://doi.org/10. 1002/mop.30628, 2017.

17. Roy, B., A. Bhattacharya, S. Mondal, et al., "Size miniaturization of microstrip antenna embedded with open-ended grounded slots," *J. Comput. Electron.*, DOI 10.1007/s10825-017-0995-6, 2017.
18. Hajlaoui, A. E., "New triple band electromagnetic band gap microstrip patch antenna with two shaped parasitic elements," *J. Comput. Electron.*, DOI 10.1007/s10825-017-1100-x, 2017.
19. Ali, T., K. D. Prasad, and R. C. Biradar, "A miniaturized slotted multiband antenna for wireless applications," *Journal of Computational Electronics*, https://doi.org/10.1007/s10825-018-1183-z, 2018.
20. Dash, R. K., P. B. Saha, D. Ghoshal, and G. Palai, "Design of triangular shaped slotted patch antennas for both wideband and multiband applications," *International Journal of Applied Electromagnetics and Mechanics*, Vol. 68, No. 3, 275–294, 2022.